View metadata, citation and similar papers at core.ac.uk

brought to you by CORE

provided by IntechOpen

We are IntechOpen, the world's leading publisher of Open Access books Built by scientists, for scientists

4,800
Open access books available

122,000
International authors and editors

135M
Downloads

154
Countries delivered to

Our authors are among the

TOP 1%
most cited scientists

12.2%
Contributors from top 500 universities

WEB OF SCIENCE™

Selection of our books indexed in the Book Citation Index in Web of Science™ Core Collection (BKCI)

Interested in publishing with us? Contact book.department@intechopen.com

Numbers displayed above are based on latest data collected.
For more information visit www.intechopen.com

29

Joystick Teaching System for Industrial Robots Using Fuzzy Compliance Control

Fusaomi Nagata, Keigo Watanabe and Kazuo Kiguchi

1. Introduction

Industrial robots have been applied to several tasks, such as handling, assembling, painting, deburring and so on (Ferretti et al., 2000), (Her & Kazerooni, 1991), (Liu, 1995), (Takeuchi et al., 1993), so that they have been spread to various fields of manufacturing industries. However, as for the user interface of the robots, conventional teaching systems using a teaching pendant are only provided. For example, in the manufacturing industry of wooden furniture, the operator has to manually input a large mount of teaching points in the case where a workpiece with curved surface is sanded by a robot sander. This task is complicated and time-consuming. To efficiently obtain a desired trajectory along curved surface, we have already considered a novel teaching method assisted by a joystick (Nagata et al., 2000), (Nagata et al., 2001). In teaching mode, the operator can directly control the orientation of the sanding tool attached to the tip of the robot arm by using the joystick. In this case, since the contact force and translational trajectory are controlled automatically, the operator has only to instruct the orientation with no anxiety about overload and non-contact state. However, it is not practical to acquire sequential teaching points with normal directions, adjusting the tool's orientation only with operator's eyes.

When handy air-driven tools are used in robotic sanding, keeping contact with the curved surface of the workpiece along the normal direction is very important to obtain a good surface quality. If the orientation of the sanding tool largely deviates from normal direction, then the kinetic friction force tends to become unstable. Consequently, smooth and uniform surface quality can't be achieved. That is the reason why a novel teaching system that assists the operator is now being expected in the manufacturing field of furniture.

In this paper, an impedance model following force control is first proposed for an industrial robot with an open architecture servo controller. The control law allows the robot to follow a desired contact force through an impedance model in Cartesian space. And, a fuzzy compliance control is also presented for an advanced joystick teaching system, which can provide the friction force acting

Open Access Database www.i-techonline.com

Source: Industrial-Robotics-Theory-Modelling-Control, ISBN 3-86611-285-8, pp. 964, ARS/plV, Germany, December 2006, Edited by: Sam Cubero

between the sanding tool and workpiece to the operator (Nagata et al., 2001). The joystick has a virtual spring-damper system, in which the component of stiffness is suitably varied according to the undesirable friction force, by using a simple fuzzy reasoning method. If an undesirable friction force occurs in teaching process, the joystick is controlled with low compliance. Thus, the operator can feel the friction force thorough the variation of joystick's compliance and recover the orientation of the sanding tool. We apply the joystick teaching using the fuzzy compliance control to a teaching task in which an industrial robot FS-20 with an open architecture servo controller profiles the curved surface of a wooden workpiece. Teaching experimental results demonstrate the effectiveness and promise of the proposed teaching system.

2. Impedance Model Following Force Control

More than two decades ago, two representative force control methods were proposed (Raibert, 1981), (Hogan, 1985) ; controllers using such methods have been advanced and further applied to various types of robots. However, in order to realize a satisfactory robotic sanding system based on an industrial robot, deeper considerations and novel designs are needed. Regarding the force control, we use the impedance model following force control that can be easily applied to industrial robots with an open architecture servo controller (Nagata et al., 2002). The desired impedance equation for Cartesian-based control of a robot manipulator is designed by

$$\boldsymbol{M}_d(\ddot{\boldsymbol{x}}-\ddot{\boldsymbol{x}}_d)+\boldsymbol{B}_d(\dot{\boldsymbol{x}}-\dot{\boldsymbol{x}}_d)+\boldsymbol{S}\boldsymbol{K}_d(\boldsymbol{x}-\boldsymbol{x}_d)=\boldsymbol{S}\boldsymbol{F}+(\boldsymbol{I}-\boldsymbol{S})\boldsymbol{K}_f(\boldsymbol{F}-\boldsymbol{F}_d) \tag{1}$$

where $\boldsymbol{x}\in\Re^3$, $\dot{\boldsymbol{x}}\in\Re^3$ and $\ddot{\boldsymbol{x}}\in\Re^3$ are the position, velocity and acceleration vectors, respectively. $\boldsymbol{M}_d\in\Re^{3\times3}$, $\boldsymbol{B}_d\in\Re^{3\times3}$ and $\boldsymbol{K}_d\in\Re^{3\times3}$ called impedance parameters are the coefficient matrices of the desired mass, damping and stiffness, respectively. $\boldsymbol{F}\in\Re^3$ is the force vector acting between the end-effector and its environment. $\boldsymbol{K}_f\in\Re^{3\times3}$ is the force feedback gain matrix. $\boldsymbol{x}_d$, $\dot{\boldsymbol{x}}_d$, $\ddot{\boldsymbol{x}}_d$ and $\boldsymbol{F}_d^T$ are the desired position, velocity, acceleration and force vector; $\boldsymbol{S}$ and $\boldsymbol{I}$ are the switch matrix diag(S_1,S_2,S_3) and identity matrix. It is assumed that $\boldsymbol{M}_d$, $\boldsymbol{B}_d$, $\boldsymbol{K}_d$ and $\boldsymbol{K}_f$ are positive definite diagonal matrices. Note that if $\boldsymbol{S}=\boldsymbol{I}$, then Eq. (1) becomes an impedance control system in all directions; whereas if $\boldsymbol{S}$ is the zero matrix, it becomes a force control system in all directions. If the force control is used in all direction, $\boldsymbol{X}=\dot{\boldsymbol{x}}-\dot{\boldsymbol{x}}_d$ gives

$$\ddot{\boldsymbol{X}}=-\boldsymbol{M}_d^{-1}\boldsymbol{B}_d\boldsymbol{X}+\boldsymbol{M}_d^{-1}\boldsymbol{K}_f(\boldsymbol{F}-\boldsymbol{F}_d) \tag{2}$$

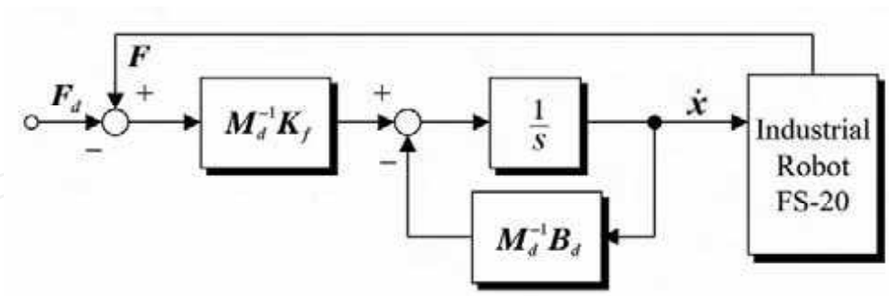

Figure 1. Block diagram of the impedance model following force control.

In general, Eq. (2) is solved as

$$\boldsymbol{X} = \exp\left(-\boldsymbol{M}_d^{-1}\boldsymbol{B}_d t\right)\boldsymbol{X}(0) + \int_0^t \exp\left\{-\boldsymbol{M}_d^{-1}\boldsymbol{B}_d(t-\tau)\right\}\boldsymbol{M}_d^{-1}\boldsymbol{K}_f(\boldsymbol{F}-\boldsymbol{F}_d)\,d\tau \tag{3}$$

Here, we will consider the form in the discrete time k using a sampling width Δt. It is assumed that $\boldsymbol{F}$ is constant within $\Delta t(k-1) \le t < \Delta tk$ and diagonal components of $\boldsymbol{M}_d$, $\boldsymbol{B}_d$, $\boldsymbol{K}_d$ and $\boldsymbol{K}_f$ are given constant values. Defining $\boldsymbol{X}(k) = \boldsymbol{X}(t)|_{t=\Delta tk}$, it follows that

$$\boldsymbol{X}(k) = \exp\left(-\boldsymbol{M}_d^{-1}\boldsymbol{B}_d\Delta t\right)\boldsymbol{X}(k-1) - \left\{\exp(-\boldsymbol{M}_d^{-1}\boldsymbol{B}_d\Delta t) - \boldsymbol{I}\right\}\boldsymbol{B}_d^{-1}\boldsymbol{K}_f\{\boldsymbol{F}(k) - \boldsymbol{F}_d\} \tag{4}$$

Remembering $\boldsymbol{X}(k) = \dot{\boldsymbol{x}}(k) - \dot{\boldsymbol{x}}_d(k)$ and setting $\dot{\boldsymbol{x}}_d(k) = 0$ in the direction of force control, a recursive equation of velocity command in Cartesian space is derived by

$$\dot{\boldsymbol{x}}(k) = \exp\left(-\boldsymbol{M}_d^{-1}\boldsymbol{B}_d\Delta t\right)\dot{\boldsymbol{x}}(k-1) - \left\{\exp(-\boldsymbol{M}_d^{-1}\boldsymbol{B}_d\Delta t) - \boldsymbol{I}\right\}\boldsymbol{B}_d^{-1}\boldsymbol{K}_f\{\boldsymbol{F}(k) - \boldsymbol{F}_d\} \tag{5}$$

where $\boldsymbol{x}(k)$ is composed of position vector $[x(k)\,y(k)\,z(k)]^T$. The manipulated variable $\dot{\boldsymbol{x}}(k)$ is given to the normal direction to a workpiece. Figure 1 shows the block diagram of the impedance model following force control in *s*-domain.

Profiling control is the basic strategy for sanding or polishing, and it is performed by both force control and position/orientation control. However, it is very difficult to realize stable profiling control under such environments that have unknown dynamics or shape. Undesirable oscillations and non-contact state tend to occur. To reduce such undesirable influences, an integral action is added to Eq. (5), which yields

$$v_f(k) = exp\left(-M_d^{-1}B_d\Delta t\right)\dot{x}(k-1) - \left\{ exp(-M_d^{-1}B_d\Delta t) - I \right\}$$
$$B_d^{-1}K_f\left\{F(k) - F_d\right\} + K_i\sum_{n=1}^{k}\left\{F(n) - F_d\right\} \tag{6}$$

where $\boldsymbol{K}_i = \mathrm{diag}(K_{i1}, K_{i2}, K_{i3})$ is the integral gain. The manipulated variable $\boldsymbol{v}_f(k)$ given by Eq. (6) is also substituted into the reference of the Cartesian based servo controller incorporated in an industrial robot, so that the contact force $\boldsymbol{F}(k)$ can track the reference $\boldsymbol{F}_d$ through the impedance model.

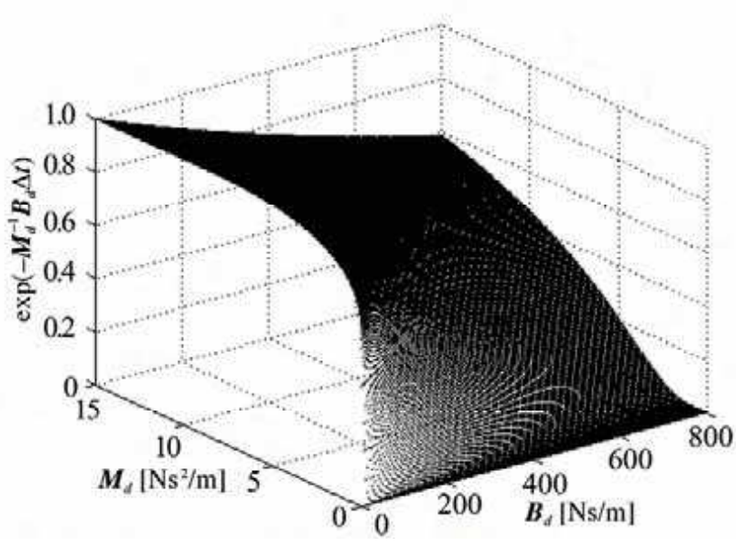

Figure 2. Relation among desired mass M_{di}, damping B_{di} and $\exp(-M_{di}^{-1}B_{di}\Delta t)$

From Eq. (6), the following characteristics are seen. Among the impedance parameters, desired damping has much influence on force control response as well as the force feedback gain. The larger $\boldsymbol{B}_d$ becomes, the smaller the effectiveness of force feedback becomes. Figure 2 shows the relation among M_{di}, B_{di} and diagonal elements of transition matrix $\exp\left(-M_{di}^{-1}B_{di}\Delta t\right)$ in the case that Δt is set to 0.01 [s]. i denotes the i-th (i=1, 2, 3) diagonal element As can be seen, for example, if B_{di} is smaller than about 100, then appropriate M_{di} is limited. M_{di} over 15 leads $\exp\left(-M_{di}^{-1}B_{di}\Delta t\right)$ to almost 1. In selecting the impedance parameters, their combinations should be noted.

3. Fuzzy Compliance Control of a Joystick Device

3.1 Fuzzy Compliance Control

In our proposed teaching system, the joystick is used to control the orientation of the sanding tool attached to the top of the robot arm. The rotational velocity of the orientation is generated based on the values of the encoder in x- and y-rotational directions as shown in Fig. 3. Also, the compliance of the joystick is varied according to the kinetic friction force acting between a sanding tool and workpiece. As the friction force becomes large, the joint of the joystick is controlled more stiffly. Therefore, the operator can perform teaching tasks having the change of the friction force with the joystick's compliance.
The desired compliance equation for the joint-based control of a joystick is designed by

$$\boldsymbol{\tau}_J = \boldsymbol{B}_J \dot{\boldsymbol{\theta}}_J + \widetilde{\boldsymbol{K}}_J \boldsymbol{\theta}_J \tag{7}$$

where $\boldsymbol{\tau}_J \in \Re^2$ is the joint driving torque vector of the joystick. $\boldsymbol{\theta}_J \in \Re^2$ and $\dot{\boldsymbol{\theta}}_J \in \Re^2$ are the inclination angle and the angular velocity vectors, respectively. $\boldsymbol{B}_J = \mathrm{diag}(B_{Jx}, B_{Jy})$ and $\widetilde{\boldsymbol{K}}_J = \mathrm{diag}(\widetilde{K}_{Jx}, \widetilde{K}_{Jy})$ are the virtual damper and stiffness matrices of the joystick joints. The subscripts x, y denotes x- and y-directional components in Fig. 3, respectively.

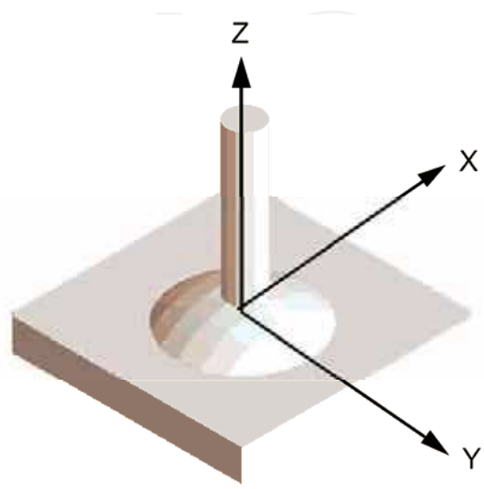

Figure 3. Coordinate system of a joystick

Further, to adjust the compliance of the joystick according to the friction force, $\widetilde{\boldsymbol{K}}_J$ is defined as

$$\begin{pmatrix} \widetilde{K}_{Jx} & 0 \\ 0 & \widetilde{K}_{Jy} \end{pmatrix} = \begin{pmatrix} K_{Jx} & 0 \\ 0 & K_{Jy} \end{pmatrix} + \begin{pmatrix} \Delta K_{Jx} & 0 \\ 0 & \Delta K_{Jy} \end{pmatrix} \tag{8}$$

where $\boldsymbol{K}_J = \mathrm{diag}(K_{Jx}, K_{Jy})$ is the base stiffness matrix, $\Delta\boldsymbol{K}_J = \mathrm{diag}(\Delta K_{Jx}, \Delta K_{Jy})$ is the compensated stiffness matrix whose diagonal elements are suitably given from the following fuzzy reasoning part.

3.2 Generation of Compensated Stiffness Using Simple Fuzzy Reasoning

In this section, we discuss how to suitably generate the compensated stiffness according to the undesirable friction force. The compensated stiffness is adjusted by using a simple fuzzy reasoning method, so that the teaching operator can conduct the teaching task delicately feeling the friction force acting between the sanding tool and workpiece through the compliance of the joystick. In teaching, x- and y-directional frictions F_x and F_y in the base coordinate system are used as fuzzy inputs for the fuzzy reasoning, and they are used to estimate y- and x-rotational compliance of the joystick joints. The present fuzzy rules are described as follows:

Rule 1: If $|F_x|$ is $\widetilde{A}_{x1}$ and $|F_y|$ is $\widetilde{A}_{y1}$, Then $\Delta K_{Jx} = B_{x1}$ and $\Delta K_{Jy} = B_{y1}$

Rule 2: If $|F_x|$ is $\widetilde{A}_{x2}$ and $|F_y|$ is $\widetilde{A}_{y2}$, Then $\Delta K_{Jx} = B_{x2}$ and $\Delta K_{Jy} = B_{y2}$

Rule 3: If $|F_x|$ is $\widetilde{A}_{x3}$ and $|F_y|$ is $\widetilde{A}_{y3}$, Then $\Delta K_{Jx} = B_{x3}$ and $\Delta K_{Jy} = B_{y3}$

$\vdots$

Rule L: If $|F_x|$ is $\widetilde{A}_{xL}$ and $|F_y|$ is $\widetilde{A}_{yL}$, Then $\Delta K_{Jx} = B_{xL}$ and $\Delta K_{Jy} = B_{yL}$

Where $\widetilde{A}_{xi}$ and $\widetilde{A}_{yi}$ are i-th (i=1,…,L) antecedent fuzzy sets for $|F_x|$ and $|F_y|$, respectively. L is the number of the fuzzy rules. B_{xi} and B_{yi} are the consequent constant values which represent i-th x- and y-rotational compensated stiffness, respectively. In this case, the antecedent confidence calculated by i-th fuzzy rule is given by

$$\omega_i = \mu_{Axi}(|F_x|) \wedge \mu_{Ayi}(|F_y|) \tag{9}$$

where $\mu_X(\cdot)$ is the Gaussian type membership function for a fuzzy set represented by

$$\mu_X(x) = \exp\left\{\log\frac{(x-\alpha)^2\beta^2}{2}\right\} \tag{10}$$

where α and β are the center of membership function and reciprocal value of standard deviation, respectively.

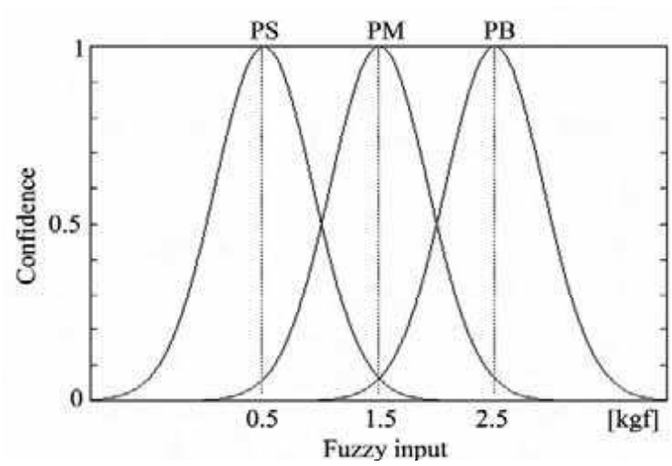

Figure 4, Antecedent membership function for $|F_x|$ and

	$\lvert F_y \rvert$		
$\lvert F_x \rvert$	PB	PM	PS
PB	$(4.0K_{Jx}, 4.0K_{Jy})$	$(3.0K_{Jx}, 4.0K_{Jy})$	$(0.4K_{Jx}, 4.0K_{Jy})$
PM	$(4.0K_{Jx}, 3.0K_{Jy})$	$(3.0K_{Jx}, 3.0K_{Jy})$	$(0.4K_{Jx}, 3.0K_{Jy})$
PS	$(4.0K_{Jx}, 0.4K_{Jy})$	$(3.0K_{Jx}, 0.4K_{Jy})$	$(0.4K_{Jx}, 0.4K_{Jy})$

Table 1. Constant values in the consequent part.

In the sequal, the compensated stiffness matrix $\Delta\boldsymbol{K}_J$ is obtained from the weighted mean method given by

$$\Delta\boldsymbol{K}_J = \mathrm{diag}\left\{\frac{\sum_{i=1}^{L} B_{xi}\omega_i}{\sum_{i=1}^{L}\omega_i}, \frac{\sum_{i=1}^{L} B_{yi}\omega_i}{\sum_{i=1}^{L}\omega_i}\right\} \tag{11}$$

Figure 4 shows the designed antecedent membership functions. On the other hand, the designed consequent constants, which represent the compensated values of the stiffness, are tabulated in Table 1. In teaching experiments, the friction force more than 3 kgf is regarded as an overload. If such an overload is detected, then the teaching task is automatically stopped and the polishing tool is immediately removed from the workpiece. Therefore, the support set of range [0, 3] in Fig. 3 is used for the antecedent part.

4. Teaching Experiment

4.1 Sanding Robot System

Throughout the remainder of this paper, the effectiveness of the proposed teaching method is proved by teaching experiments.

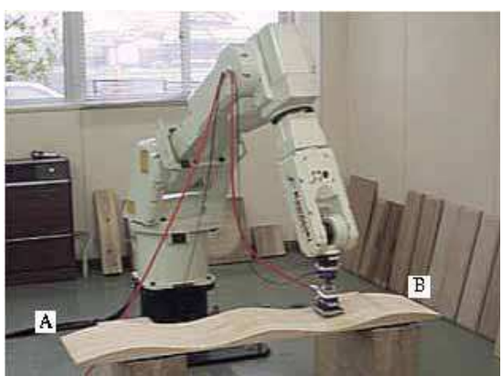

Photo 1. Robotic sanding system.

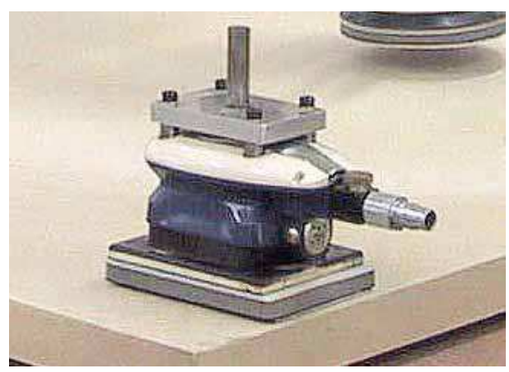

Photo 2 Air-driven sanding tool.

Photo 3. Joystick system used in teaching experiments (Impulse Engine2000).

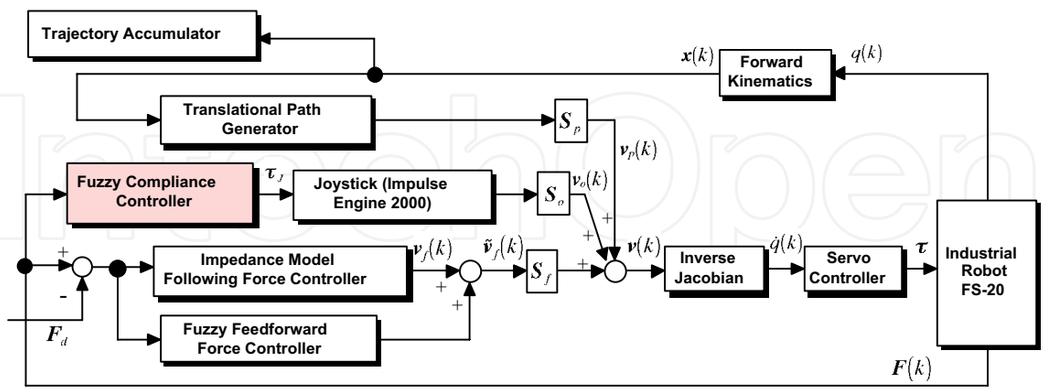

Figure 5. Block diagram of the sanding robot in teaching mode.

Photo 1 shows the overview of the sanding robot used in the teaching experiments. The base 6-DOF industrial robot with an open architecture servo controller is the model FS-20 provided by Kawasaki Heavy Industries, whose tip of the arm has an air-driven sanding tool as shown in Photo 2 via a 6-DOF force/torque sensor 67M25A provided by Nitta corporation. The permitted weight of workpieceis under 20 kgf. The size of the sanding tool is 60 × 100 mm^2 and its paper roughness is #120. Since this type of tool tends to cause not only high frequency but also large magnitude vibrations, we use the force sensor's filter whose cutoff frequency is set to 30 Hz. Photo 3 shows the 2-DOF joystick Impulse Engine2000 provided by Immersion corporation. This joystick can perform a maximum force of 8.9 N by controlling the joint torque with 2048 steps. In teaching experiments, we apply the fuzzy compliance control given by Eq. (7) to this joystick.

Figure 5 shows the block diagram of the sanding robot in teaching mode. The proposed teaching process is as follows: in the direction of position control, the translational trajectory generator yields a base trajectory such as a zigzag path and whirl path with a velocity command $\boldsymbol{v}_p(k)$. In the direction of orientation control, a rotational velocity $\boldsymbol{v}_o(k)$ is generated using the compensated angle of inclination $\tilde{\boldsymbol{\theta}}_J = \left[\tilde{\theta}_{Jx}\ \tilde{\theta}_{Jy}\right]^T$ with a valocity transformation gain $\boldsymbol{K}_v$. $\tilde{\theta}_{Ji}$ (i = x, y) is obtained by

$$\tilde{\theta}_{Ji} = \begin{cases} 0 & \text{if} \quad -500 \le \theta_{Ji} \le 500 \\ \theta_{Ji} - 500 & \text{if} \quad \theta_{Ji} > 500 \\ \theta_{Ji} + 500 & \text{if} \quad \theta_{Ji} < -500 \end{cases} \tag{12}$$

Note that $\boldsymbol{\theta}_J = [\theta_{Jx}\ \theta_{Jy}]^T$ in Eqs. (12) and (7) are the same variable. In this case, the teaching operator can conduct the teaching task feeling the friction force acting between the sanding tool and workpiece with the compliance of the joystick. In the direction of force control, the impedance model following force controller given by Eq. (6) yields $\boldsymbol{v}_f(k)$, in which $\boldsymbol{v}_f(k)$ is added to the output from the already proposed fuzzy feedforward force controller (Nagata et al., 1999) to generate $\tilde{\boldsymbol{v}}_f(k)$. After switched by S_p, S_o and S_f, each directional velocity command is summed up to compose a velocity vector $\boldsymbol{v}(k)$. $\boldsymbol{v}(k)$ is transformed into a joint angle velocity $\dot{\boldsymbol{q}}(k)$ with the inverse Jacobian to give to the servo controller.

4.2 Teaching Experiments

In order to examine the effectiveness of the proposed teaching system, an experiment as shown in Photo 1 was conducted using a workpiece machined by a 5-axis NC machine tool. Figure 6 shows the CAD model of the workpiece. The teaching was carried out under the following conditions: the air power of the sanding tool is switched off; the profiling velocity in the tangent direction is set to 20 mm/s; the desired contact force in the normal direction is set to 1 kgf; and the sanding tool moves from the point A to the point B in Photo 1.

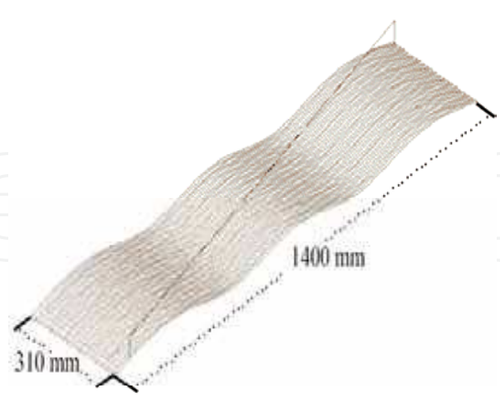

Figure 6. CAD Model of a workpiece

Photo 1. Teaching scene by using the proposed system

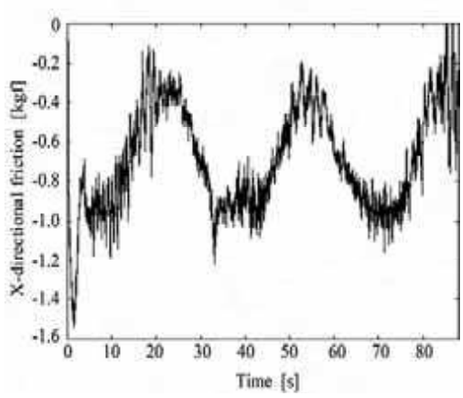

Figure 7. X-directional friction force

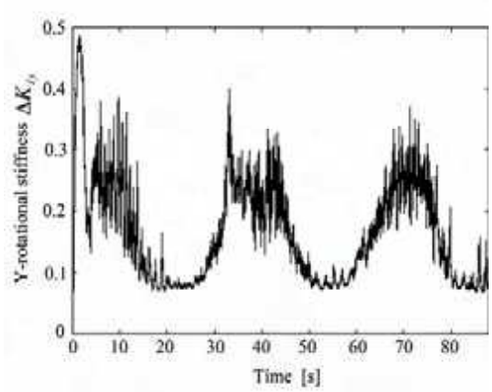

Figure 8. Y-rotational stiffnes generated by fuzzy resoning

The base compliance of the joystick is set to $K_{Jx} = K_{Jy}$ =0.167, $B_{Jx} = B_{Jy}$ =0.5. Table 2 shows the control parameters given in the experiment. After these preparations, an experiment on the proposed joystick teaching was done. Photo 4 shows the teaching scene by using the proposed teaching system. Figures 7 and 8 show x-directional friction force f_x and y-rotational component ΔK_{Jy} of the compensated stiffness matrix $\Delta \boldsymbol{K}_J$, respectively.

Desired contact force $\sqrt{(F_x)^2 + (F_z)^2}$	1 [kgf]
Desired mass coefficient M_{d1}, M_{d3}	0.01 [kgf·s^2/mm]
Desired damping coeficinet B_{d1}, B_{d3}	10 [kgf·s/mm]
Force feedback gain K_{f1}, K_{f3}	1
Angle velocity gain K_{vx}, K_{vy}	0.03
Profiling velocity $\lvert v_p \rvert$	20 [mm/s]
Sampling width Δt	10 [msec]

Table 2. Designed control parameters in teaching mode

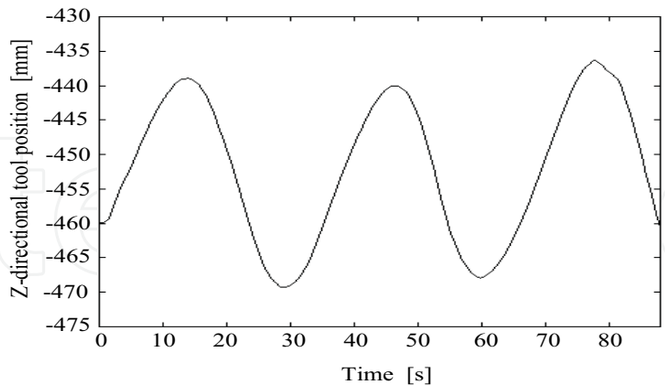

Figure 9. Obtained tip position in the *z*-direction

It is observed from the result that the compliance of the joystick changes according to the friction acting between the sanding tool and workpiece. Thus, the operator could execute the teaching task feeling the friction force with the compliance of the joystick. In teaching, the time series data of both the position and orientation were stored into the trajectory accumulator as shown in Fig. 5. Figure 9 shows the *z*-directional position obtained by this teaching.

4.3 Sanding Task Using the Acquired Trajectory

Figure 10 shows the block diagram of the sandinging robot in playback mode. An experiment on polishing task was carried out using the acquired trajectory. In this case, although the tangent profiling velocity was set to 40 mm/s which was two times as fast as that in teaching mode, the polishing task could be stably practiced. The *z*-directional force control result is plotted in Fig. 11.

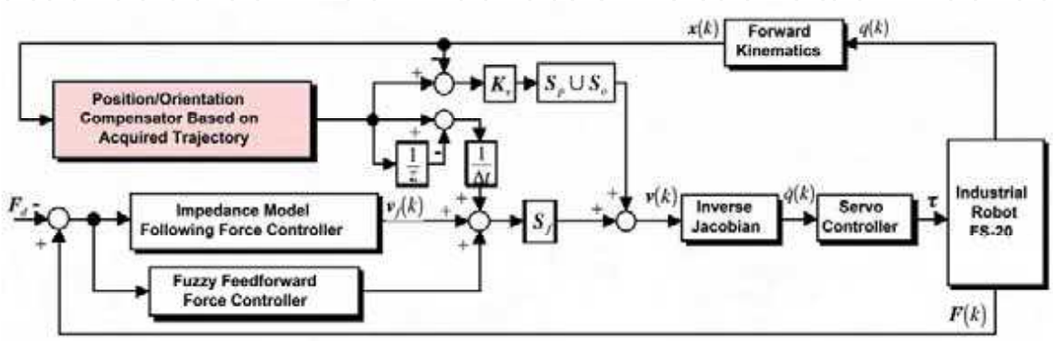

Figure 10. Block diagram of sending robot in diagram in playback mode using joystick taught data.

It has been observed that a desirable response is obtained in spite of tool's large vibrations. Furthermore, the surface accuracy of the workpiece was so good condition as well as polished by skilled workers. The measurements evaluated by arithmetical mean roughness method were less than 2μm.

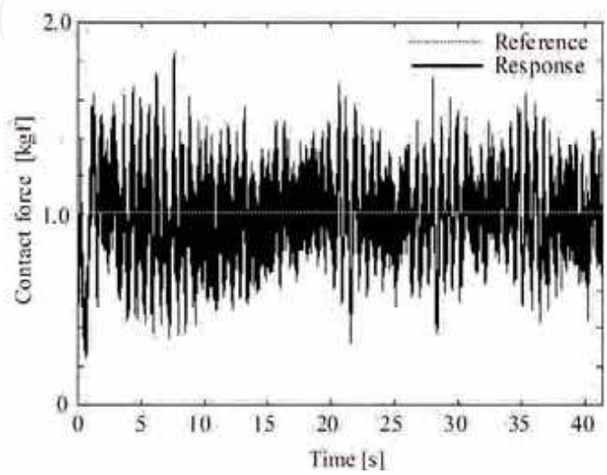

Figure 11. Force control result in playback mode

5. Conclusion

In this paper, a joystick teaching system using a fuzzy compliance control has been proposed for industrial robots. We have applied the proposed teaching system to a teaching task of a furniture sanding robot. Experimentally, it was demonstrated that the operator could safely carry out the teaching task feeling the friction force acting between a sanding tool and workpiece through the compliance of the joystick.

The proposed teaching process is as follows: first, a zigzag path considered according to both sizes of each work and sanding tool is prepared; next, the sanding robot, in which an impedance model following force control method is incorporated, profiles the surface of the workpiece along the zigzag path. The operator has only to control the orientation of the sanding tool using the fuzzy compliance controlled joystick so that the tool and workpiece can be in contact each other keeping the desired relation of position and orientation. Since the force controller keeps the contact force a desired value, the operator has to give no attention to a sudden over-load or non-contact state. The desired trajectory is automatically obtained as the data including continuous information of the position and orientation along the zigzag path on the workpiece surface. In playback mode, the robot can finally achieve the sanding task without any assists of the operator by referring the acquired trajectory.

6. References

Ferretti, G.; Magnani, G. & Rocco, P. (2000). Triangular Force/Position Control with Application to Robotic Deburring, *Machine Intelligence & Robotic Control*, Vol. 2, No. 2, pp. 83-91.

Her, M. & Kazerooni, H. (1991). Automated Robotic Deburring of Parts Using Compliance Control, *ASME Journal of Dynamic systems, Measurement, and Control*, Vol. 113, pp. 60-66.

Hogan, N. (1985). Impedance Control: An Approach to Manipulation, *Trans. ASME, J. Dyn. Syst. Measure. Contr.*, Vol. 107, pp. 1–24.

Liu, M. H. (1995). Force-Controlled Fuzzy-Logic-Based Robotic Deburring, *Control Engineering Practice*, Vol. 3, No. 2, pp. 189-201.

Nagata, F.; Watanabe, K. & Izumi, K. (1999). Position-Based Impedance Control Using a Fuzzy Compensator, *Procs. of the 3rd International Conference on Knowledge-Based Intelligent Information Engineering Systems (KES'99)*, pp. 125-128.

Nagata, F.; Watanabe, K.; Hashino, S.; Tanaka, H.; Matsuyama, T. & Hara, K. (2000). Polishing Robot Using a Joystick Controlled Teaching System, *CD-ROM Procs. of the IEEE International Conference on Industrial Electronics, Control and Instrumentation (IECON-2000)*, pp. 632-637.

Nagata, F.; Watanabe, K.; Hashino, S.; Tanaka, H.; Matsuyama, T. & Hara, K. (2001). Polishing Robot Using Joystick Controlled Teaching, *Journal of Robotics and Mechatronics*, Vol. 13, No. 5, pp. 517-525.

Nagata, F.; Watanabe, K.; Kiguchi, K.; Tsuda, K.; Kawaguchi, S.; Noda, Y. & Komino, M. (2001). Joystick Teaching System for Polishing Robots Using Fuzzy Compliance Control, *Procs. of 2001 IEEE International Symposium on Computational Intelligence in Robotics and Automation*, pp. 362-367.

Nagata, F.; Watanabe, K.; Fujimoto, Y.; Kiguchi, K. & Murase, Y. (2002). 3D Machining and Finishing System for New Designed Furniture, *Procs. of 2002 Japan-USA Symposium on Flexible Automation*, pp. 1239-1245.

Raibert, M. H. & Craig, J. J. (1981). Hybrid Position/Force Control of Manipulators, *Trans. ASME, J. Dyn. Syst. Measure. Contr.*, Vol. 102, pp. 126–133.

Takeuchi, Y.; Ge, D. & Asakawa, N. (1993). Automated Polishing Process with a Human-like Dexterous Robot, *Procs. of IEEE International Conference Robotics and Automation*, pp. 950-956.

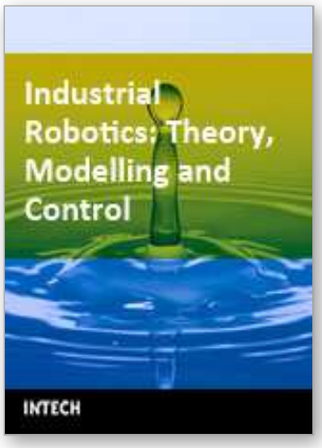

Industrial Robotics: Theory, Modelling and Control

Edited by Sam Cubero

ISBN 3-86611-285-8

Hard cover, 964 pages

Publisher Pro Literatur Verlag, Germany / ARS, Austria

Published online 01, December, 2006

Published in print edition December, 2006

This book covers a wide range of topics relating to advanced industrial robotics, sensors and automation technologies. Although being highly technical and complex in nature, the papers presented in this book represent some of the latest cutting edge technologies and advancements in industrial robotics technology. This book covers topics such as networking, properties of manipulators, forward and inverse robot arm kinematics, motion path-planning, machine vision and many other practical topics too numerous to list here. The authors and editor of this book wish to inspire people, especially young ones, to get involved with robotic and mechatronic engineering technology and to develop new and exciting practical applications, perhaps using the ideas and concepts presented herein.

How to reference

In order to correctly reference this scholarly work, feel free to copy and paste the following:

Fusaomi Nagata, Keigo Watanabe and Kazuo Kiguchi (2006). Joystick Teaching System for Industrial Robots Using Fuzzy Compliance Control, Industrial Robotics: Theory, Modelling and Control, Sam Cubero (Ed.), ISBN: 3-86611-285-8, InTech, Available from:
http://www.intechopen.com/books/industrial_robotics_theory_modelling_and_control/joystick_teaching_system_for_industrial_robots_using_fuzzy_compliance_control

INTECH
open science | open minds

InTech Europe
University Campus STeP Ri
Slavka Krautzeka 83/A
51000 Rijeka, Croatia
Phone: +385 (51) 770 447
Fax: +385 (51) 686 166
www.intechopen.com

InTech China
Unit 405, Office Block, Hotel Equatorial Shanghai
No.65, Yan An Road (West), Shanghai, 200040, China
中国上海市延安西路65号上海国际贵都大饭店办公楼405单元
Phone: +86-21-62489820
Fax: +86-21-62489821

© 2006 The Author(s). Licensee IntechOpen. This chapter is distributed under the terms of the Creative Commons Attribution-NonCommercial-ShareAlike-3.0 License, which permits use, distribution and reproduction for non-commercial purposes, provided the original is properly cited and derivative works building on this content are distributed under the same license.